

# Biodistribution and environmental safety of a live-attenuated YF17D-vectorized SARS-CoV-2 vaccine candidate

Li-Hsin Li,<sup>1</sup> Laurens Liesenborghs,<sup>1,6,7</sup> Lanjiao Wang,<sup>2,7</sup> Marleen Lox,<sup>3</sup> Michael Bright Yakass,<sup>1,4</sup> Sander Jansen,<sup>1</sup> Ana Lucia Rosales Rosas,<sup>2</sup> Xin Zhang,<sup>1</sup> Hendrik Jan Thibaut,<sup>5</sup> Dirk Teuwen,<sup>1</sup> Johan Neyts,<sup>1</sup> Leen Delang,<sup>2</sup> and Kai Dallmeier<sup>1</sup>

<sup>1</sup>KU Leuven, Department of Microbiology, Immunology and Transplantation, Rega Institute for Medical Research, Laboratory of Virology and Chemotherapy, Molecular Vaccinology and Vaccine Discovery Team, 3000 Leuven, Belgium; <sup>2</sup>KU Leuven, Department of Microbiology, Immunology and Transplantation, Rega Institute for Medical Research, Laboratory of Virology and Chemotherapy, Mosquito Virology Team, 3000 Leuven, Belgium; <sup>3</sup>KU Leuven, Department of Cardiovascular Sciences, Centre for Molecular and Vascular Biology, 3000 Leuven, Belgium; <sup>4</sup>University of Ghana, Department of Biochemistry, Cell and Molecular Biology, the West African Centre for Cell Biology of Infectious Pathogens (WACCBIP), Legon, Accra 1181, Ghana; <sup>5</sup>KU Leuven, Department of Microbiology, Immunology and Transplantation, Rega Institute for Medical Research, Translational Platform Virology and Chemotherapy (TPVC), 3000 Leuven, Belgium; <sup>6</sup>Institute of Tropical Medicine, Department of Clinical Sciences, Outbreak Research Team, 2000 Antwerp, Belgium

**New platforms are needed for the design of novel prophylactic vaccines and advanced immune therapies. Live-attenuated yellow fever vaccine YF17D serves as a vector for several licensed vaccines and platform for novel candidates. On the basis of YF17D, we developed an exceptionally potent COVID-19 vaccine candidate called YF-S0. However, use of such live RNA viruses raises safety concerns, such as adverse events linked to original YF17D (yellow fever vaccine-associated neurotropic disease [YEL-AND] and yellow fever vaccine-associated viscerotropic disease [YEL-AVD]). In this study, we investigated the biodistribution and shedding of YF-S0 in hamsters. Likewise, we introduced hamsters deficient in signal transducer and activator of transcription 2 (STAT2) signaling as a new preclinical model of YEL-AND/AVD. Compared with YF17D, YF-S0 showed improved safety with limited dissemination to brain and visceral tissues, absent or low viremia, and no shedding of infectious virus. Considering that yellow fever virus is transmitted by *Aedes* mosquitoes, any inadvertent exposure to the live recombinant vector via mosquito bites is to be excluded. The transmission risk of YF-S0 was hence compared with readily transmitting YF-Asibi strain and non-transmitting YF17D vaccine, with no evidence for productive infection of mosquitoes. The overall favorable safety profile of YF-S0 is expected to translate to other vaccines based on the same YF17D platform.**

## INTRODUCTION

Roughly 2 years after its first emergence in 2019–2020, more than 5 million people have succumbed to coronavirus disease 2019 (COVID-19), caused by severe acute respiratory syndrome coronavirus 2 (SARS-CoV-2) (<https://coronavirus.jhu.edu/map.html>). Mass immunization is key to mitigating the expanding pandemic.<sup>1</sup> A set

of rapidly developed prophylactic vaccines plays a crucial role in global immunization against SARS-CoV-2. Several of these vaccines are first in class, based on novel platforms, including game-changer mRNA vaccines and viral vector vaccines that are unprecedented in both their high clinical efficacy and the incremental advance in breakthrough innovation.<sup>2–4</sup> However, a global vaccine supply shortage, the dependence on an ultra-cold chain system in case of mRNA vaccines, and the continuous emergence of virus variants pose unmet challenges.<sup>5,6</sup> Unfortunately, the long-term effectiveness of current SARS-CoV-2 vaccines is waning because of the combined effect of (1) a rapid decay of virus-neutralizing antibodies (nAbs) over time and (2) emergence of new variants escaping vaccine-induced immunity.<sup>7–9</sup> Furthermore, several first-generation COVID-19 vaccines have a rather high reactogenicity. With the growing number of vaccinated people, more cases and a wider spectrum of adverse effects following immunization (AEFI), including severe adverse effects (SAEs) such as myocarditis and life-threatening deep-venous thrombosis, are described.<sup>10–15</sup> In summary, there is an urgent need to develop new and improved second-generation COVID-19 vaccines to eliminate the pandemic.

Recently, we used an alternative vaccine platform that uses the fully replication-competent live-attenuated yellow fever (YF) vaccine YF17D as a vector<sup>16</sup> and developed a virus-vectorized SARS-CoV-2

Received 3 January 2022; accepted 14 March 2022;  
<https://doi.org/10.1016/j.omtm.2022.03.010>.

<sup>7</sup>These authors contributed equally

**Correspondence:** Kai Dallmeier, PhD, KU Leuven, Department of Microbiology, Immunology and Transplantation, Rega Institute for Medical Research, Laboratory of Virology and Chemotherapy, Molecular Vaccinology and Vaccine Discovery Team, 3000 Leuven, Belgium.

**E-mail:** [kai.dallmeier@kuleuven.be](mailto:kai.dallmeier@kuleuven.be)



vaccine candidate (YF-S0) that expresses a stabilized prefusion form of SARS-CoV-2 spike protein (S0).<sup>17</sup> YF-S0 was shown to induce vigorous humoral and cellular immune responses in hamsters (*Mesocricetus auratus*), mice (*Mus musculus*), and cynomolgus macaques (*Macaca fascicularis*) and was able to prevent COVID-19-like disease after single-dose vaccination in a stringent hamster model. Because of its YF17D backbone, YF-S0 could serve as dual vaccine to also prevent yellow fever virus (YFV) infections, which should provide an added benefit for populations living in regions at risk for YFV outbreaks.<sup>18</sup>

In addition to preclinical efficacy, development of such a new vaccine requires in-depth evaluations of its safety to support progression from preclinical study to clinical trials. In particular for live-attenuated viral vaccines such as YF-S0, the biodistribution of the vaccine virus after administration needs to be assessed<sup>19</sup> to understand the viral organ tropism and hence to exclude potential direct harm to specific tissues. Our vaccine candidate, YF-S0, showed an excellent safety profile in multiple preclinical models, including in non-human primates (NHPs) and interferon-deficient mice and hamsters.<sup>17</sup> However, use of such a recombinant YF17D vaccine entails some potential concerns.<sup>19</sup> In particular, replication and persistence of YF-S0 in tissues and body fluids pose a theoretical risk for YF vaccine-associated viscerotropic disease (YEL-AVD) and YF vaccine-associated neurotropic disease (YEL-AND), which are originally linked to parental YF17D.<sup>20</sup> With this regard, parental YF17D vaccine is commonly used as benchmark for direct comparison in safety assessment.<sup>19</sup>

Here, we investigated the biodistribution and shedding of YF-S0 following vaccination in hamsters, with the following aims: (1) to understand to what extent YF-S0 causes viremia resulting in virus dissemination to vital organs; (2) to evaluate the risks of YF-S0 for YEL-AVD/AND by confirming its transient and self-limited replication *in vivo*,<sup>17</sup> restricting the risks for YEL-AVD/AND; and (3) to determine to what extent viral RNA remains detectable in body secretions and, if so, (4) whether this poses any environment risks for shedding of recombinant infectious virus. Furthermore, YFV is a mosquito-borne virus, and YF-S0 uses YFV-derived YF17D as a vector. Recombinant YF-S0 might hence, though highly attenuated, pose an environmental risk due to unforeseen phenotypical changes. Taking this theoretical consideration into account, we tested the infectivity of YF-S0 on *Aedes aegypti* (*Ae. aegypti*) mosquitoes to assess its transmission potential. *Ae. aegypti* was selected as target mosquito species because of its well-known high vector competence for YFV.<sup>21</sup> It is well documented that wild-type YF-Asibi can infect and disseminate in *Ae. aegypti*, while YF17D only occasionally infects the midgut and is unable to disseminate to secondary organs.<sup>22,23</sup> Therefore, these two YFV strains were used as controls to assess transmission of YF-S0 by a competent vector.

Finally, we corroborate the favorable safety profile of YF-S0 by reporting limited dissemination and shedding in vaccinated hamsters and no risk for mosquito-borne transmission.

## RESULTS

### Tissue distribution of YF-S0 and parental YF17D in hamsters

For our assessment, we chose wild-type (WT) Syrian golden hamsters as a preferred small animal model of YFV infection<sup>24</sup> and injected them with a high dose ( $10^4$  plaque-forming units [PFU]) of either YF17D (n = 6) or YF-S0 (n = 6) via the intraperitoneal (i.p.) route to achieve maximal exposure; primary pharmacodynamics have been previously documented<sup>17</sup> and are confirmed here by consistently high seroconversion rates (at least 80%) to YFV-specific nAbs (Figure S1). Likewise, a  $10^4$  PFU i.p. dose was shown to elicit saturating levels of SARS-CoV-2 nAbs in the hamster model, similar to a two-dose regimen using a 10-fold lower inoculum.<sup>17</sup> As methods control, we inoculated STAT2 knockout (STAT2<sup>-/-</sup>) hamsters with  $10^4$  PFU YF17D (n = 2). STAT2<sup>-/-</sup> hamsters are deficient in antiviral type I and type III interferon responses<sup>25</sup> and therefore prone to uncontrolled flavivirus replication.<sup>26</sup> Tissues sampled for analysis were chosen on the basis of biodistribution data available from non-human primates and humans. In macaques, detection of YF17D RNA has been reported in lymph nodes, spleen, and liver at 7 days after subcutaneous inoculation.<sup>27</sup> Likewise, viral RNA is widespread and abundantly found in spleen, liver, brain, kidney, and other organs in patients who developed YEL-AVD.<sup>20,28</sup> On the basis of this knowledge, we collected spleen, liver, brain, and kidney as the most common target organs to assess the risks for YEL-AVD and YEL-AND. Ileum and parotid gland were collected as additional excretory tissues and lung as the main target of COVID-19 (Figure 1A). From our previous experience,<sup>17</sup> we observed that the replication of YF17D or YF-S0 is transient and well tolerated in WT hamsters. Tissue analysis in hamsters was thus performed 7 days post-inoculation (dpi) (i.e., a few days after peak of viremia), in line with similar studies performed for chimeric YF17D vaccine in macaques before<sup>27</sup> and at a time point at which STAT2<sup>-/-</sup> hamsters needed to be euthanized for humane reasons.<sup>17</sup>

Viral RNA above detection limits in YF17D-vaccinated WT hamsters was mostly limited to spleen (RNA detected in 4 of 6 animals), with the exception of a single hamster in which viral RNA was widespread to the brain, parotid gland, and lung (Figure 1B; Table S1). Detection of YF-S0 was markedly less frequent and restricted to only kidney (2 of 6) and lung (1 of 6) (Figure 1B). Overall, in either group RNA level was low and barely detectable by sensitive RT-qPCR, indicative for limited replication in WT hamsters. In contrast, unrestricted replication of virus to high viral loads was observed in STAT2<sup>-/-</sup> hamsters (Figures 1B and 1C). Importantly, no viral RNA nor infectious virus could be detected in the brains of YF-S0-vaccinated hamsters, suggesting a low associated YEL-AND risk (Figures 1D and 1E).

Viremia is considered a key indicator for the risk for developing YEL-AVD. Thus, longitudinal blood sampling was conducted as shown in Figure 2A. Kinetics of viral RNA in serum as proxy for viremia have been reported earlier for WT hamsters vaccinated with YF17D or YF-S0<sup>17</sup> and are discussed here in comparison with respective data from STAT2<sup>-/-</sup> controls (Figure 2B). Viremia

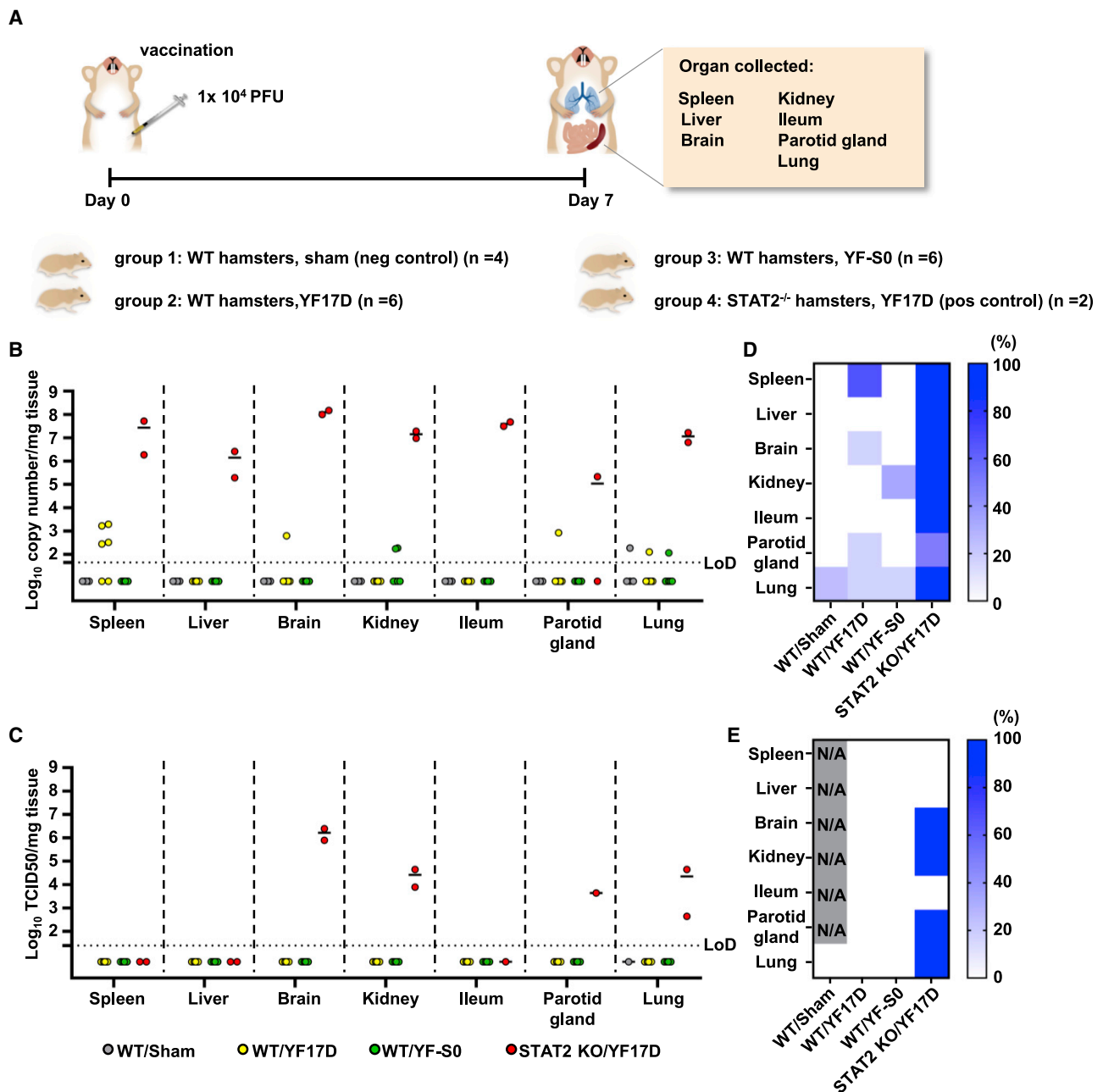


**Figure 1. Biodistribution of YF-S0 in hamsters**

(A) Schematic of hamster vaccination and organ collection. Hamsters were inoculated i.p. with  $10^4$  PFU/mL of either YF17D or YF-S0 and sacrificed 7 days later. Organs from 4 different experimental groups, including sham-vaccinated wild-type (WT) hamsters and YF17D-vaccinated  $STAT2^{-/-}$  (knockout [KO]) hamsters as respective negative and positive controls, were collected and divided for RNA extraction and virus isolation. (B) Viral RNA load by RT-qPCR. (C) Virus isolation by  $TCID_{50}$  assay. For sham and  $STAT2$  KO, only PCR-positive samples were analyzed. (D and E) Heatmap representing positivity rates by organ and experimental group on the basis of the results of RT-qPCR (D) or  $TCID_{50}$  assay (E). Bars in (B) and (C) represent median values. N/A, not applicable.

could be detected consistently in all YF17D-vaccinated WT hamsters (6 of 6) starting at 1 dpi and lasting for a median of 2.5 days (95% confidence interval, 1–4 days); in contrast, viral RNA was detected only once at 3 dpi in a single YF-S0-vaccinated

hamster (1 of 6) (Figure 2B; Table S2). In  $STAT2^{-/-}$  hamsters, YF17D grew unrestrictedly to markedly increased viral RNA levels (Figure 2B), readily detectable by virus isolation (Figure S2). Integration of data over the course of immunization (area under the

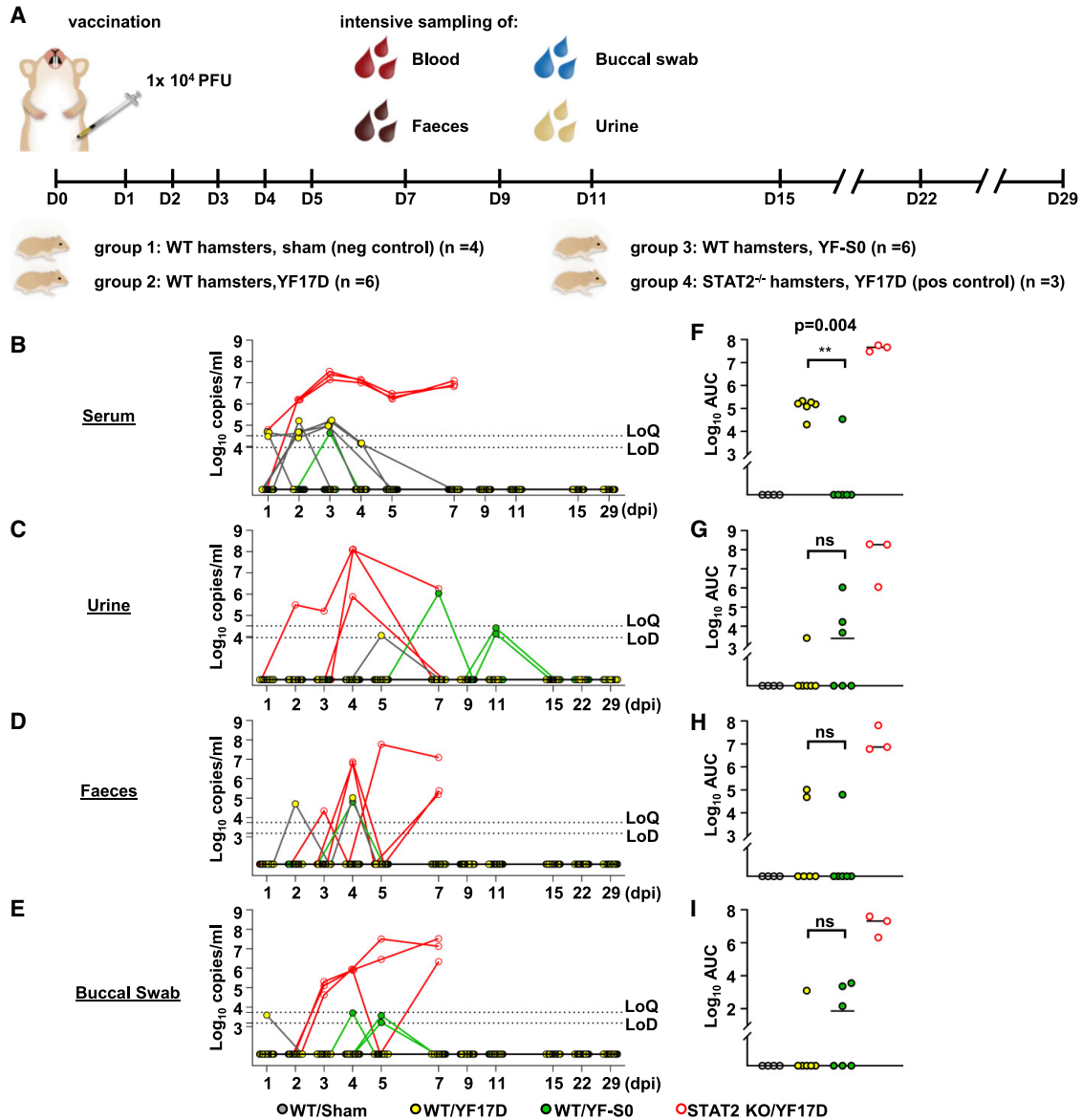


**Figure 2. Shedding of YF-S0 by vaccinated hamsters**

(A) Schematic of vaccination and specimen collection. Hamsters were inoculated as in Figure 1A, and serum, urine, feces, and buccal swabs were serially sampled at indicated time points. (B–E) Viral RNA load by RT-qPCR. (F–I) Area under curve (AUC; copies × day) calculated in GraphPad Prism 8; the Mann-Whitney test was used for the statistical analysis, with  $p > 0.05$  marked as non-significant (ns); and  $**p \leq 0.01$ . Serum RNA data for YF17D and YF-S0-vaccinated WT hamsters as previously published. LoQ, limit of quantification; LoD, limit of detection; dpi, days post-inoculation.

curve [AUC]) indicated a significant reduced overall serum virus load in YF-S0-vaccinated animals (Figure 2F).

#### Limited shedding of YF-S0 and parental YF17D RNA

As shedding of viral RNA in urine after YF17D vaccination has been reported,<sup>29</sup> we sampled different body fluids to investigate respective virus levels (Figure 2A). Within all longitudinally sampled specimens, viral RNA was detected only sporadically in urine (1 of 56 and 3 of 58), feces (2 of 65 and 1 of 66), and buccal swabs (1 of 66 and 3 of

66) of both YF17D and YF-S0-vaccinated hamsters, respectively, mostly at very low copy numbers and not linked to viremia (Figures 2C–2E and S3; Table S3–S5). Noteworthy, viral RNA could be detected, if at all, only within the first 11 dpi, clearly indicating that viral replication was self-limiting, leading to the final elimination of the live viral vector from all tissues. Also, there was no significant difference in AUC between both groups (Figures 2G–2I). The potential risk that YF-S0 could be spread through excrement of vaccinated individuals should hence be as low as for YF17D. In addition, no viable

virus could be isolated from urine samples, with RNA counts as high as  $10^8$  copies/mL (not shown), in line with no clinical evidence for secondary spread in urine, matching long-standing field experience for YF17D.

#### Abortive infection of YF-S0 on yellow fever virus-competent vector *Ae. aegypti*

YF-S0 is derived from mosquito-borne YFV, and human-to-human transmission by a competent mosquito vector could theoretically lead to unintentional exposure to the vaccine, including in immune-compromised people.<sup>30</sup> Thus, the transmission risk of YF-S0 should be excluded regarding main indicators of mosquito vector competence<sup>21,31,32</sup> (Figure 3A): (1) sufficient virus ingestion from infectious blood meal, (2) productive infection of virus in mosquito midgut (midgut infection barrier [MIB]), and (3) virus escapes from midgut barrier (MEB) (i.e., dissemination to parenteral tissues to establish sufficiently high virus loads in salivary glands to enable transmission). To this end, *Ae. aegypti* mosquitoes, as the species of YFV-competent vector,<sup>21</sup> were given infectious blood meals with no virus, YF17D, YF-S0, or wild-type YF-Asibi strain as positive control.<sup>22,23</sup> Samples as collected on day 0 in whole mosquitoes (ingestion step), on day 14 in thorax and abdomen (virus infection and replication in mosquito midgut; marked as main body), and on day 14 in head, legs, and wings (dissemination) were determined using both RT-qPCR and a CPE-based assay (50% tissue culture infective dose [TCID<sub>50</sub>]) for virus infection and replication (Figure 3A). Considering the relatively long extrinsic incubation period of YFV<sup>21</sup> in mosquitoes and particularly that of YF17D,<sup>23</sup> earlier time points were not considered for analysis.

Experimental feeding was equally efficient for all three virus groups regarding both viral RNA and infectious virus recovered (Figures 3B and 3C). However, 14 days after feeding, viral RNA was detected exclusively in specimens from the YF17D group (8 of 15) and YF-Asibi group (8 of 23) but none from the YF-S0 group. Importantly, infectious viral particles were detectable only in the YF-Asibi group, with virus loads as high as about  $10^6$  TCID<sub>50</sub>/body on average (Figure 3C). For dissemination beyond the MEB, the remaining head, legs, and wings of each six virus-positive mosquitoes with highest body virus loads from the YF17D and YF-Asibi groups, respectively, and six randomly chosen specimens from the YF-S0 group were evaluated. All these specimens from the YF-Asibi group (6 of 6) scored positive for dissemination, compared with none from the YF-S0 or YF17D groups (Figures 3B and 3C). These results suggest that YF-S0 is able neither to pass the MIB for midgut infection nor to escape from the midgut (MEB) for dissemination (Figures 3D and 3E).

## DISCUSSION

The live-attenuated YF17D vaccine is considered one of the most powerful and successful vaccines and has been used in humans for decades.<sup>33</sup> Its well-known characteristics of stimulating both vigorous humoral and cellular immune responses, as well as favorable innate responses, are of interest for other vaccine targets using the YF17D

genome as a backbone.<sup>16</sup> We recently generated a particularly potent YF17D-vectored vaccine candidate, YF-S0, against SARS-CoV-2 infection, inserting the non-cleavable spike protein of SARS-CoV-2 (S0) between the E and NS1 region of YF17D.<sup>17</sup> This construct serves as antigens to induce vigorous immune responses against both SARS-CoV-2 and YFV infections.<sup>17</sup>

Apart from YF-S0, YF17D is currently the only fully replication-competent viral vector that is part of any licensed recombinant live viral vaccine in wide use for human medicine, that is, in the two licensed human vaccines, JE-CV (against Japanese encephalitis; Imojev<sup>34</sup>) and CYD-TDV (against all four serotypes of dengue virus; Dengvaxia<sup>35</sup>). Additional YF17D-based vaccine candidates are in different stages of (pre)clinical development, including vaccines against other flaviviruses (West Nile virus: ChimeriVax-WN02<sup>36</sup>; Zika virus: YF-ZIKprM/E<sup>37</sup>) or non-flaviviruses (HIV: rYF17D/SIV-Gag45-269<sup>38</sup>; Lassa virus: YFV17D/LASV-GPC<sup>39</sup>; chronic hepatitis B virus: YF17D/HBc-C<sup>40</sup>). Like other YF17D-vectored vaccines, YF-S0 triggers vigorous protective immune responses, including high levels of SARS-CoV-2 neutralizing antibodies after single-dose vaccination in hamsters, mice, and cynomolgus macaques.<sup>17</sup> However, all these YF17D-vectored vaccines share the theoretical concerns of SAEs associated with the parental YF17D vaccine, such as YEL-AVD (0.4 per 100,000) and YEL-AND (0.8 per 100,000),<sup>19,20,41,42</sup> notably despite little (pre)clinical evidence or reports from post-marketing surveillance.<sup>43</sup> In contrast, though originally contraindicated in more vulnerable people, such as children, pregnant women, people living with HIV or diabetes, and older persons, growing evidence now suggests increased risk from YF17D.<sup>44,45</sup>

To temper the safety concerns, the viscerotropism and neurovirulence of YF-S0 were compared head-to-head with parental YF17D virus by investigating the biodistribution and viremia following administration of either vaccine virus in hamsters. We demonstrate that parental YF17D can spread systemically and viral RNA can be detected in the spleen, brain, parotid gland, and lung in YF17D-vaccinated WT hamsters. However, replication of YF17D remains restricted, resulting in infectious virus loads below detection limits. Compared with YF17D, detection of YF-S0 was further limited, with minute amounts of viral RNA in the kidney and lung. Unrestricted virus replication to high viral loads as cause of viscerotropic or neurotropic disease was observed only in STAT2<sup>-/-</sup> hamsters, in line with the essential role innate interferon signaling plays in live vaccines<sup>30,46</sup> and control of viral infections in general.<sup>47</sup> In addition, in YF-S0-vaccinated WT hamsters, detection of viremia was rare (Figure 2B) and, importantly, less frequent (1 of 6) and markedly lower in magnitude (AUC) and duration (1 day) compared with parental YF17D (6 of 6 for >2 days). A limitation of our study may be the relatively small number of animals enrolled per group and the finite number of time points selected for analysis. However, taken together, the overall limited tissue distribution of YF-S0 as well as the low abundance of its RNA in blood, below detection limits for infectious virus, suggest a further lowered risk for YEL-AVD/AND for YF-S0 than that reported parental YF17D. It is thus to be decided to what extent such highly



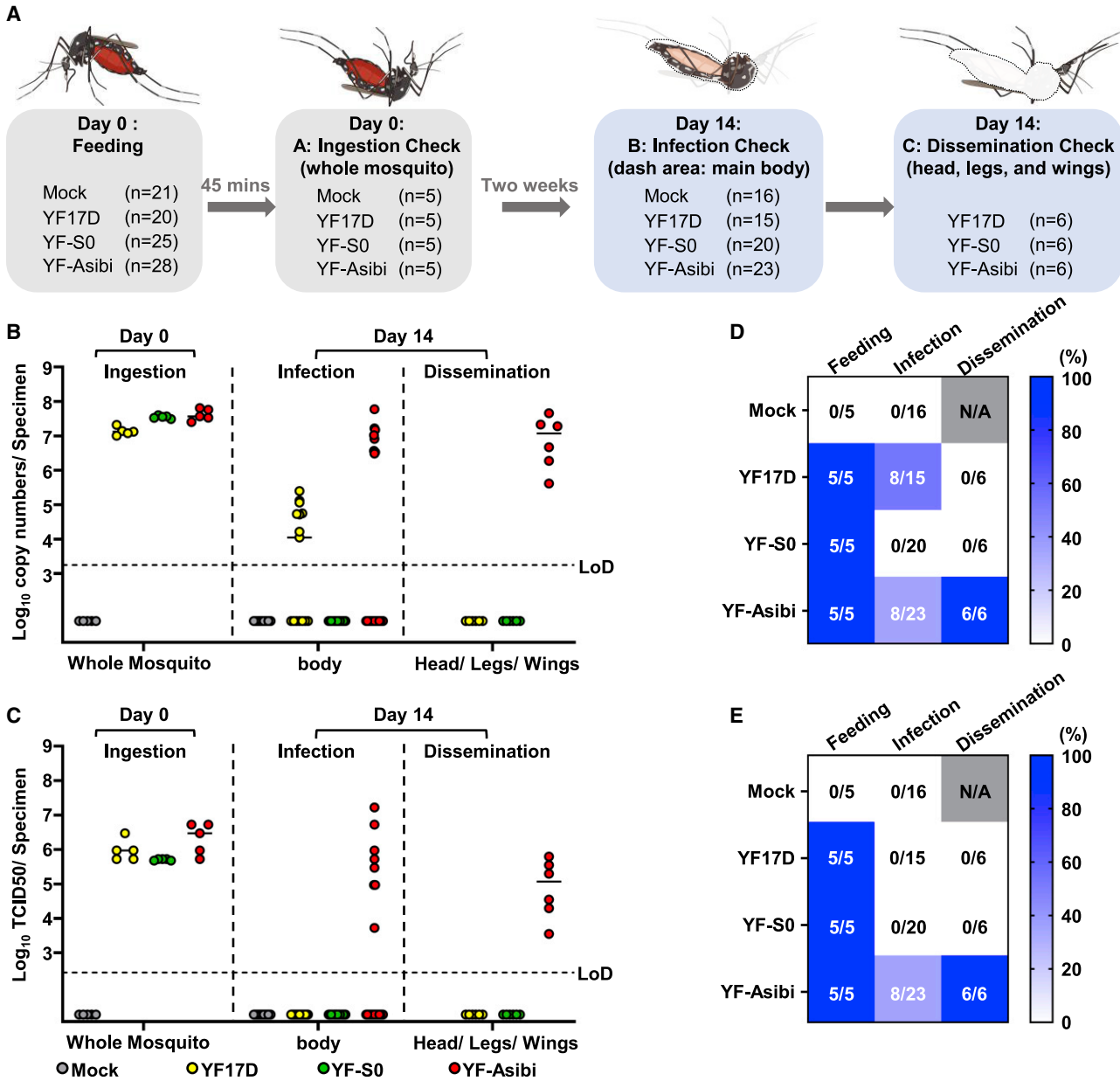


**Figure 3. Assessment of YF-S0 transmission potential by *Aedes* mosquitoes**

(A) Schematic of virus feeding of mosquitoes and specimen collection. Mosquitoes were fed with infectious blood meal containing YF17D, YF-S0, YF-Asibi, or mock. Five mosquitoes were collected each for ingestion assessment. At 14 days post-feeding (dpf), remaining mosquitoes were dissected into two parts, midgut (infection assessment) and head, legs, and wings (dissemination assessment). (B) Viral RNA load by RT-qPCR. (C) Virus isolation by TCID<sub>50</sub> assay. For assessment of ingestion and infection, RT-qPCR and TCID<sub>50</sub> were performed on all samples. For assessment of dissemination, only a selection of PCR-positive specimens from the YF17D and YF-Asibi groups (n = 6 each) were further analyzed using TCID<sub>50</sub> assay, plus 6 randomly chosen from the YF-S0 group. (D and E) Heatmap representing positivity rates per experiment group as scored by RT-qPCR (D) and TCID<sub>50</sub> assay (E). Bars in (B) and (C) represent median values. N/A, not applicable. Mosquito icons were adapted from BioRender.com.

attenuated recombinant YF17D-vectored vaccines need to fulfill all World Health Organization (WHO) requirements for original yellow fever vaccine,<sup>48</sup> including monkey neurovirulence test as previously endorsed.<sup>19</sup>

To further investigate the potential environment risk associated with shedding of recombinant virus, we collected urine, feces, and buccal swabs from vaccinated hamsters and checked for the presence of viral RNA for 29 days to determine how long YF-S0 would remain

detectable in body secretions compared with YF17D. No significant differences in vaccine RNA shedding were observed between YF17D and YF-S0 during the course of immunization (Figures 2G–2I, AUC). Importantly, no infectious virus could be isolated, suggesting the risk is very low, even if any inadvertent exposure by vaccinated individuals to their environment. In summary, these results obtained in a hamster model of YF vaccination clearly demonstrate that (1) the overall viral tissue burden for YF-S0 was considerably lower than for parental YF17D, and (2) presence of viral RNA in body secretions (urine, feces, and buccal swab) was equally low as for YF17D, mostly likely void of residual infectious virus particles. YF-S0 vaccine virus infection is transient and harbors minimal, if at all any, risk for shedding or evidence for environmental biosafety concern.

Last, though the chances of YF17D-vectored vaccines to be transmitted by arthropod vectors are minimal, we evaluated the replication competence of YF-S0 in yellow fever mosquito vector (i.e., *Ae. aegypti*). Although parental YF17D passed the MIB and was restricted at the MEB as previously documented,<sup>22,23</sup> YF-S0 was already blocked at the first barrier, with no remaining viral RNA or infectious virus detectable after an infectious bloodmeal. Hence, the transmissibility of YF-S0 by mosquitoes is to be considered neglectable.

Altogether, YF-S0 can be considered a safe and efficacious vaccine candidate for the prevention of COVID-19. A similar improved safety compared with parental YF17D can be expected for other vaccines following the same design principle (i.e., using transgenic, yet fully replication-competent YF17D as a vector).<sup>16,40</sup>

## MATERIALS AND METHODS

### Animal experiment

#### Hamsters

Wild-type outbred specific pathogen-free Syrian hamsters (*Mesocricetus auratus*) were purchased from Janvier Laboratories (France). The generation<sup>49</sup> and characterization<sup>25</sup> of STAT2<sup>-/-</sup> (gene identifier: 101830537) hamsters has been described elsewhere. STAT2<sup>-/-</sup> hamsters were bred in-house. Hamsters (maximum n = 2) were housed in individually ventilated cages (Sealsafe Plus, Tecniplast; cage type GR900), under standard conditions of 21°C, 55% humidity, and 12 :12 h light/dark cycles. Hamsters were provided food and water ad libitum, as well as extra bedding material and wooden gnawing blocks for enrichment as previously described. This project was approved by the KU Leuven ethics committee (P015-2020), following institutional guidelines approved by the Federation of European Laboratory Animal Science Associations (FELASA). Hamsters were euthanized by intraperitoneal administration of 500  $\mu$ L (hamsters) Dolethal (200 mg/mL sodium pentobarbital; V  toquinol SA).

#### Vaccine and virus stocks

Vaccine viruses used throughout this study have been described.<sup>17</sup> YF-S0 was derived from a cDNA clone of YF17D (GenBank: X03700) with an in-frame insertion of a non-cleavable version of the SARS-CoV-2 S protein (GenBank: MN908947.3) in the YFV E/NS1 intergenic region. YF-S0 vaccine stocks were grown on baby

hamster kidney (BHK21) cells. The molecular and antigenic structure and replication of YF-S0 have been described in detail.<sup>17</sup> Original YF17D vaccine (Stamaril, Sanofi-Pasteur; lot number G5400) was purchased via the pharmacy of the University Hospital Leuven and passaged twice in Vero E6 cells prior to use.

For the construction of YF-Asibi, the cDNA of YF17D sequence in plasmid pShuttle/YF17D<sup>50</sup> was adjusted to match previously described molecular YF-Asibi clone Ap7M (GenBank: MF926243) by using standard recombinant DNA technology. The respective cDNA was custom synthesized (IDT, Belgium) as six partially overlapping fragments (averaging 2 kb in size) and assembled by homologous recombination in yeast, *S. cerevisiae*. The thus obtained plasmid pShuttle/Ap7M was transfected into BHK-21J cells for virus rescue. The virus stock was prepared by passaging twice in BHK-21J cells, and the genome of YF-Asibi virus was confirmed by direct sequencing. All virus titers were determined by plaque assay on BHK-21J cells as before.<sup>17</sup>

#### Biodistribution

WT hamsters (6–8 weeks old, female) were inoculated intraperitoneally with a 10<sup>4</sup> PFU/mL dose of YF17D (n = 6) or YF-S0 (n = 6). STAT2<sup>-/-</sup> hamsters (6–8 weeks old, female) were inoculated intraperitoneally with 10<sup>4</sup> PFU/mL of YF17D (n = 2). At 7 dpi, blood, spleen, liver, brain, kidney, ileum, parotid gland, and lung were collected.

#### Shedding

WT hamsters (6–8 weeks old, female) were inoculated intraperitoneally with 10<sup>4</sup> PFU/mL of YF17D (n = 6) or YF-S0 (n = 6). STAT2<sup>-/-</sup> hamsters (6–8 weeks old, male) were inoculated intraperitoneally with 10<sup>4</sup> PFU/mL of YF17D (n = 3). Blood, urine, feces, and buccal swab were collected daily for the first 5 dpi, then every other day until 11 dpi and 15, 22 (except for the blood) and 29 dpi, and afterward once a week until 29 dpi.

#### Mosquito experiment

##### Mosquito strain

*Ae. aegypti* Paea<sup>51</sup> were obtained via the Infravec2 consortium (<https://infravec2.eu/product/live-eggs-or-adult-females-of-aedes-aegypti-strain-paea-2/>) from Institute Pasteur of Paris. Mosquitoes were maintained at the insectary of Rega Institute, and the fourth generation was used for this study. In brief, larvae were fed with yeast tablets (Gayelord Hauser, France) until the pupae stage prior to transfer to cages for emergence. Adults were maintained with cotton soaked in 10% sucrose solution under standard conditions (28°C, 80% relative humidity, and 14 h:10 h light/dark cycle).

#### Oral infection and sample collection

Seven-day-old female mosquitoes were starved 24 h prior to infection. Infectious blood meals contained rabbit erythrocytes plus 5 mM adenosine triphosphate as phagostimulant, supplemented with virus stocks to final titers of 2  $\times$  10<sup>5</sup> PFU/mL for both YF17D and YF-S0, and 5  $\times$  10<sup>6</sup> PFU/mL for YF-Asibi, respectively.

After 45 min, five fully engorged females from each group were frozen for viral input assessment (ingestion check; Figure 3A), and the rest were kept with 10% of sugar solution under both controlled conditions ( $28 \pm 1^\circ\text{C}$ , relative humidity 80%, light/dark cycle 14 h:10 h, supplied with 10% sucrose solution) and BSL-3 containment conditions. At 14 dpi, mosquitoes were dissected into two parts; main body (thorax and abdomen) and remainder, collected individually in tubes containing PBS and 2.8 mm ceramic beads (Precellys). The samples were homogenized and pass through 0.8  $\mu\text{m}$  column filters (Sartorius, Germany). Thus, cleared supernatants were used for TCID<sub>50</sub> assay or kept at  $-80^\circ\text{C}$  for RNA extraction and subsequent RT-qPCR analysis.

### RNA extraction

Solid tissues (organs), feces, and buccal swabs were homogenized in a bead mill (Precellys) in lysis buffer (catalog no. 740984.10; Macherey-Nagel). After homogenization, samples were centrifuged at 10,000 rpm for 5 min to remove cell debris, and total RNA was extracted by using NucleoSpin Plus RNA virus Kit (catalog no. 740984.10; Macherey-Nagel). For serum (50  $\mu\text{L}$ ), urine (50  $\mu\text{L}$ ) and homogenates of mosquito samples (150  $\mu\text{L}$ ), NucleoSpin RNA virus kit (catalog no. 740956.250; Macherey-Nagel) was used for RNA extraction.

### RT-qPCR

RT-qPCR for YFV detection was performed as previously described<sup>17</sup> using primers and probe targeting the YFV NS3 gene<sup>23</sup> on an ABI 7500 Fast Real-Time PCR System (Applied Biosystems). Absolute quantification was based on standard curves generated from 5-fold serial dilutions of YF17D cDNA with a known concentration.

### TCID<sub>50</sub> assay

For virus isolation and quantification BHK21 cells were infected with 10-fold serial dilutions in 96-well plates and incubated at  $37^\circ\text{C}$  for 6 days using DMEM with 2% fetal bovine serum (Hyclone), 2 mM L-glutamine (Gibco), 1% sodium bicarbonate (Gibco), and 1% antibiotics (PenStrep) as assay medium. Solid tissues were homogenized in a bead mill (Precellys) in assay medium and centrifuged at 10,000 rpm for 5 min ( $4^\circ\text{C}$ ) to remove debris. Resulting viral titers were calculated using the Reed and Muench method.

### Serum neutralization test

Titers of YFV-specific neutralizing antibodies were determined using BHK21 cells and a mCherry-tagged variant of YF17D virus (YFV-mCherry) as described.<sup>17</sup> In brief, YFV-mCherry was mixed and incubated with serial diluted of sera for 1 h at  $37^\circ\text{C}$  and subsequently transferred to BHK21 cells grown in 96-well plates for infection. At 3 days post-infection, the relative infection rate was quantified by counting mCherry-expressing cells versus total cells on a high-content screening platform (CX5, Thermo Fisher Scientific), normalizing the infection rate of untreated virus controls as 100%. Half-maximal serum neutralizing titers (SNT<sub>50</sub>) were determined by curve fitting in GraphPad Prism 8.

### Statistics

Data were analyzed using GraphPad Prism 8. Results are represented as individual values and median for summary statistics. Statistical significance was determined using non-parametric Mann-Whitney U test (\* $p \leq 0.05$  and \*\* $p \leq 0.01$ ; ns, not significant).

### SUPPLEMENTAL INFORMATION

Supplemental information can be found online at <https://doi.org/10.1016/j.omtm.2022.03.010>.

### ACKNOWLEDGMENTS

We thank Thibault Francken, Dagmar Buyst, Niels Cremers, Birgit Voeten, and Jasper Rymenants for their technical support on specimens' preparation and virus titration as well as Jasmine Paulissen for her technical assistance on generating serology data. The graphical abstract was created using [BioRender.com](https://www.biorender.com). This work was supported by project grants from the European Union's Horizon 2020 Research and Innovation Program under grant agreements 733176 (RABYD-VAX to K.D. and J.N.) and 101003627 (SCORE to J.N.). Funding was provided by the Research Foundation Flanders (FWO) under the Excellence of Science (EOS) program (30981113, VirEOS to K.D. and J.N.), the FWO COVID-19 call (G0G4820N), and by the KU Leuven/UZ Leuven COVID-19 Fund (COVAX-PREC project). L.-H.L. acknowledges support from a PhD scholarship grant from the KU Leuven Special Research Fund (DBOF/14/062). L.L. is a member of the Institute of Tropical Medicine's Outbreak Research Team, which is financially supported by the Department of Economy, Science and Innovation (EWI) of the Flemish Government. X.Z. was supported by a PhD scholarship grant from the China Scholarship Council (CSC; 201906170033). L.D. received funding from KU Leuven Internal Funds (C22/18/007 and STG/19/008) as well as K.D. (C3/19/057 Lab of Excellence). This publication was supported by the Infrac2 project, which has received funding from the European Union's Horizon 2020 Research and Innovation Program 2020 (grant agreement 731060).

### AUTHOR CONTRIBUTIONS

Overall Conceptual Design, L.-H.L., L.L., D.T., and K.D.; Methodology: L.-H.L., L.L., L.W.; *In Vivo* Experiments (Hamsters), L.L. and M.L.; *In Vivo* Experiments (Mosquitoes), L.W. and A.L.R.R.; *In Vitro* Experiments, L.-H.L. and X.Z.; *In Vitro* Experiment (Serology), H.J.T.; Design and Generation of YF-Asibi, M.B.Y. and S.J.; Data Management and Analysis: L.-H.L. and L.L.; Writing – Original Draft, L.-H.L.; Writing – Review & Editing: L.-H.L., L.L., L.W., L.D., D.T., and K.D.; Supervision, J.N. and K.D.; Funding Acquisition, J.N. and K.D.

### DECLARATION OF INTERESTS

The authors declare no competing interests.

### REFERENCES

- Dallmeier, K., Meyfroidt, G., and Neyts, J. (2021). COVID-19 and the intensive care unit: vaccines to the rescue. *Intensive Care Med.* 47, 1–4.



2. Heinz, F.X., and Stiasny, K. (2021). Distinguishing features of current COVID-19 vaccines: knowns and unknowns of antigen presentation and modes of action. *npj Vaccin.* 6, 1–13.
3. Verbeke, R., Lentacker, I., De Smedt, S.C., and Dewitte, H. (2021). The dawn of mRNA vaccines: the COVID-19 case. *J. Controlled Release* 333, 511–520.
4. Neukirch, L., Fougereux, C., Andersson, A.-M.C., and Holst, P.J. (2020). The potential of adenoviral vaccine vectors with altered antigen presentation capabilities. *Expert Rev. Vaccin.* 19, 25–41.
5. Anderson, R.M., Vegvari, C., Truscott, J., and Collyer, B.S. (2020). Challenges in creating herd immunity to SARS-CoV-2 infection by mass vaccination. *The Lancet* 396, 1614–1616.
6. Garcia-Beltran, W.F., Lam, E.C., Denis, K.S., Nitido, A.D., Garcia, Z.H., Hauser, B.M., Feldman, J., Pavlovic, M.N., Gregory, D.J., and Poznansky, M.C. (2021). Multiple SARS-CoV-2 variants escape neutralization by vaccine-induced humoral immunity. *Cell* 184, 2372–2383.e2379.
7. Cromer, D., Steain, M., Reynaldi, A., Schlub, T.E., Wheatley, A.K., Juno, J.A., Kent, S.J., Triccas, J.A., Khoury, D.S., and Davenport, M.P. (2021). Neutralising antibody titres as predictors of protection against SARS-CoV-2 variants and the impact of boosting: a meta-analysis. *The Lancet Microbe*. [https://doi.org/10.1016/S2666-5247\(21\)00337-2](https://doi.org/10.1016/S2666-5247(21)00337-2).
8. Cai, C., Liu, Y., Zeng, S., Shen, H., and Han, Y. (2021). The efficacy of COVID-19 vaccines against the B.1.617.2 (delta) variant. *Mol. Ther.* 29, 2890–2892.
9. Lai, C.-C., Chen, I.-T., Chao, C.-M., Lee, P.-I., Ko, W.-C., and Hsueh, P.-R. (2021). COVID-19 vaccines: concerns beyond protective efficacy and safety. *Expert Rev. Vaccin.* 20, 1013–1025.
10. Cai, C., Peng, Y., Shen, E., Huang, Q., Chen, Y., Liu, P., Guo, C., Feng, Z., Gao, L., and Zhang, X. (2021). A comprehensive analysis of the efficacy and safety of COVID-19 vaccines. *Mol. Ther.* 29, 2794–2805.
11. Rosenblum, H.G., Hadler, S.C., Moulia, D., Shimabukuro, T.T., Su, J.R., Tepper, N.K., Ess, K.C., Woo, E.J., Mba-Jonas, A., and Alimchandani, M. (2021). Use of COVID-19 vaccines after reports of adverse events among adult recipients of janssen (johnson & johnson) and mRNA COVID-19 vaccines (Pfizer-BioNTech and moderna): update from the advisory committee on immunization practices—United States. *Morbidity Mortality Weekly Rep.* 70, 1094.
12. Lai, C.-C., Ko, W.-C., Chen, C.-J., Chen, P.-Y., Huang, Y.-C., Lee, P.-I., and Hsueh, P.-R. (2021). COVID-19 vaccines and thrombosis with thrombocytopenia syndrome. *Expert Rev. Vaccin.* 20, 1027–1035.
13. Tobaiqy, M., MacLure, K., Elkout, H., and Stewart, D. (2021). Thrombotic adverse events reported for Moderna, Pfizer and Oxford-AstraZeneca COVID-19 vaccines: comparison of occurrence and clinical outcomes in the EudraVigilance database. *Vaccines* 9, 1326.
14. Schultz, N.H., Sørvoll, I.H., Michelsen, A.E., Munthe, L.A., Lund-Johansen, F., Ahlen, M.T., Wiedmann, M., Aamodt, A.-H., Skattør, T.H., and Tjønnfjord, G.E. (2021). Thrombosis and thrombocytopenia after ChAdOx1 nCoV-19 vaccination. *New Engl. J. Med.* 384, 2124–2130.
15. Witberg, G., Barda, N., Hoss, S., Richter, I., Wiessman, M., Aviv, Y., Grinberg, T., Auster, O., Dagan, N., and Balicer, R.D. (2021). Myocarditis after Covid-19 vaccination in a large health care organization. *New Engl. J. Med.* 385, 2132–2139.
16. Bonaldo, M.C., Sequeira, P.C., and Galler, R. (2014). The yellow fever 17D virus as a platform for new live attenuated vaccines. *Hum. Vaccin. Immunother.* 10, 1256–1265.
17. Sanchez-Felipe, L., Verduynde, T., Sharma, S., Ma, J., Lemmens, V., Van Looveren, D., Javarappa, M.P.A., Boudewijns, R., Malengier-Devlies, B., and Liesenborghs, L. (2021). A single-dose live-attenuated YF17D-vectored SARS-CoV-2 vaccine candidate. *Nature* 590, 320–325.
18. Hansen, C.A., and Barrett, A.D. (2021). The present and future of yellow fever vaccines. *Pharmaceuticals* 14, 891.
19. Monath, T.P., Seligman, S.J., Robertson, J.S., Guy, B., Hayes, E.B., Condit, R.C., Excler, J.L., Mac, L.M., Carbery, B., and Chen, R.T. (2015). Live virus vaccines based on a yellow fever vaccine backbone: standardized template with key considerations for a risk/benefit assessment. *Vaccine* 33, 62–72.
20. Barrett, A.D., and Teuwen, D.E. (2009). Yellow fever vaccine—how does it work and why do rare cases of serious adverse events take place? *Curr. Opin. Immunol.* 21, 308–313.
21. de Lataillade, L.d.G., Vazeille, M., Obadia, T., Madec, Y., Mousson, L., Kamgang, B., Chen, C.-H., Failloux, A.-B., and Yen, P.-S. (2020). Risk of yellow fever virus transmission in the Asia-Pacific region. *Nat. Commun.* 11, 1–10.
22. McGee, C.E., Tsatsarkin, K., Vanlandingham, D.L., McElroy, K.L., Lang, J., Guy, B., Decelle, T., and Higgs, S. (2008). Substitution of wild-type yellow fever asibi sequences for 17D vaccine sequences in ChimeriVax—dengue 4 does not enhance infection of *Aedes aegypti* mosquitoes. *J. Infect. Dis.* 197, 686–692.
23. Danet, L., Beauclair, G., Berthet, M., Moratorio, G., Gracias, S., Tangy, F., Choumet, V., and Jouvenet, N. (2019). Midgut barriers prevent the replication and dissemination of the yellow fever vaccine in *Aedes aegypti*. *PLoS Negl. Trop. Dis.* 13, e0007299.
24. Julander, J.G. (2016). Animal models of yellow fever and their application in clinical research. *Curr. Opin. Virol.* 18, 64–69.
25. Boudewijns, R., Thibaut, H.J., Kaptein, S.J., Li, R., Vergote, V., Seldeslachts, L., Van Weyenbergh, J., De Keyser, C., Bervoets, L., and Sharma, S. (2020). STAT2 signaling restricts viral dissemination but drives severe pneumonia in SARS-CoV-2 infected hamsters. *Nat. Commun.* 11, 1–10.
26. Siddharthan, V., Van Wettene, A.J., Li, R., Miao, J., Wang, Z., Morrey, J.D., and Julander, J.G. (2017). Zika virus infection of adult and fetal STAT2 knock-out hamsters. *Virology* 507, 89–95.
27. Monath, T.P., Liu, J., Kanasa-Thanan, N., Myers, G.A., Nichols, R., Deary, A., McCarthy, K., Johnson, C., Ermak, T., and Shin, S. (2006). A live, attenuated recombinant West Nile virus vaccine. *Proc. Natl. Acad. Sci. U S A* 103, 6694–6699.
28. Quaresma, J.A., Pagliari, C., Medeiros, D.B., Duarte, M.L., and Vasconcelos, P.F. (2013). Immunity and immune response, pathology and pathologic changes: progress and challenges in the immunopathology of yellow fever. *Rev. Med. Virol.* 23, 305–318.
29. Domingo, C., Yactayo, S., Agbenu, E., Demanou, M., Schulz, A.R., Daskalow, K., and Niedrig, M. (2011). Detection of yellow fever 17D genome in urine. *J. Clin. Microbiol.* 49, 760–762.
30. Hernandez, N., Bucciol, G., Moens, L., Le Pen, J., Shahrooei, M., Goudouris, E., Shirvani, A., Changi-Ashtiani, M., Rokni-Zadeh, H., and Sayar, E.H. (2019). Inherited IFNAR1 deficiency in otherwise healthy patients with adverse reaction to measles and yellow fever live vaccines. *J. Exp. Med.* 216, 2057–2070.
31. Franz, A.W., Kantor, A.M., Passarelli, A.L., and Clem, R.J. (2015). Tissue barriers to arbovirus infection in mosquitoes. *Viruses* 7, 3741–3767.
32. Kramer, L.D., and Ciota, A.T. (2015). Dissecting vectorial capacity for mosquito-borne viruses. *Curr. Opin. Virol.* 15, 112–118.
33. Pulendran, B. (2009). Learning immunology from the yellow fever vaccine: innate immunity to systems vaccinology. *Nat. Rev. Immunol.* 9, 741–747.
34. Appaihari, M.B., and Vrtati, S. (2012). Clinical development of IMOJEV®—a recombinant Japanese encephalitis chimeric vaccine (JE-CV). *Expert Opin. Biol. Ther.* 12, 1251–1263.
35. Guy, B., Noriega, F., Ochiai, R.L., L'azou, M., Delore, V., Skipetrova, A., Verdier, F., Coudeville, L., Savarino, S., and Jackson, N. (2017). A recombinant live attenuated tetravalent vaccine for the prevention of dengue. *Expert Rev. Vaccin.* 16, 671–684.
36. Biedenbender, R., Bevilacqua, J., Gregg, A.M., Watson, M., and Dayan, G. (2011). Phase II, randomized, double-blind, placebo-controlled, multicenter study to investigate the immunogenicity and safety of a West Nile virus vaccine in healthy adults. *J. Infect. Dis.* 203, 75–84.
37. Kum, D.B., Boudewijns, R., Ma, J., Mishra, N., Schols, D., Neyts, J., and Dallmeier, K. (2020). A chimeric yellow fever-Zika virus vaccine candidate fully protects against yellow fever virus infection in mice. *Emerging microbes & infections* 9, 520–533.
38. Bonaldo, M.C., Martins, M.A., Rudersdorf, R., Mudd, P.A., Sacha, J.B., Piaskowski, S.M., Costa Neves, P.C.C., Veloso de Santana, M.G., Vojnov, L., and Capuano, S., III (2010). Recombinant yellow fever vaccine virus 17D expressing simian immunodeficiency virus SIVmac239 gag induces SIV-specific CD8+ T-cell responses in rhesus macaques. *J. Virol.* 84, 3699–3706.
39. Bredenbeek, P.J., Molenkamp, R., Spaan, W.J., Deubel, V., Marianneau, P., Salvato, M.S., Moshkoff, D., Zapata, J., Tikhonov, I., and Patterson, J. (2006). A recombinant

- Yellow Fever 17D vaccine expressing Lassa virus glycoproteins. *Virology* 345, 299–304.
40. Boudewijns, R., Ma, J., Neyts, J., and Dallmeier, K. (2021). A novel therapeutic hepatitis B vaccine candidate induces strong polyfunctional cytotoxic T cell responses in mice. *JHEP Rep.* 100295.
  41. Monath, T.P. (2012). Review of the risks and benefits of yellow fever vaccination including some new analyses. *Expert Rev. Vaccin.* 11, 427–448.
  42. Lindsey, N.P., Rabe, I.B., Miller, E.R., Fischer, M., and Staples, J.E. (2016). Adverse event reports following yellow fever vaccination, 2007–13. *J. Trav. Med.* 23, taw045.
  43. Ma, H.-Y., Lai, C.-C., Chiu, N.-C., and Lee, P.-I. (2020). Adverse events following immunization with the live-attenuated recombinant Japanese encephalitis vaccine (IMOJEV®) in Taiwan, 2017–18. *Vaccine* 38, 5219–5222.
  44. Thomas, R.E., Lorenzetti, D.L., Spragins, W., Jackson, D., and Williamson, T. (2012). The safety of yellow fever vaccine 17D or 17DD in children, pregnant women, HIV+ individuals, and older persons: systematic review. *Am. J. Trop. Med. Hyg.* 86, 359.
  45. Rafferty, E., Duclos, P., Yactayo, S., and Schuster, M. (2013). Risk of yellow fever vaccine-associated viscerotropic disease among the elderly: a systematic review. *Vaccine* 31, 5798–5805.
  46. Bastard, P., Michailidis, E., Hoffmann, H.-H., Chbihi, M., Le Voyer, T., Rosain, J., Philippot, Q., Seeleuthner, Y., Gervais, A., and Materna, M. (2021). Auto-antibodies to type I IFNs can underlie adverse reactions to yellow fever live attenuated vaccine. *J. Exp. Med.* 218, e20202486.
  47. Schoggins, J.W. (2019). Interferon-stimulated genes: what do they all do? *Annu. Rev. Virol.* 6, 567–584.
  48. Ferguson, M., Shin, J., Knezevic, I., Minor, P., and Barrett, A. (2010). WHO Working Group on technical specifications for manufacture and evaluation of yellow fever vaccines. *Vaccine* 28, 8236–8245.
  49. Fan, Z., Li, W., Lee, S.R., Meng, Q., Shi, B., Bunch, T.D., White, K.L., Kong, I.-K., and Wang, Z. (2014). Efficient gene targeting in golden Syrian hamsters by the CRISPR/Cas9 system. *PLoS One* 9, e109755.
  50. Kum, D.B., Mishra, N., Vrancken, B., Thibaut, H.J., Wilder-Smith, A., Lemey, P., Neyts, J., and Dallmeier, K. (2019). Limited evolution of the yellow fever virus 17d in a mouse infection model. *Emerging Microbes Infections* 8, 1734–1746.
  51. Vazeille-Falcoz, M., Mousson, L., Rodhain, F., Chungue, E., and Failloux, A.-B. (1999). Variation in oral susceptibility to dengue type 2 virus of populations of *Aedes aegypti* from the islands of Tahiti and Moorea, French Polynesia. *Am. J. Trop. Med. Hyg.* 60, 292–299.